



# UNIVERSITÀ DI PARMA

## ARCHIVIO DELLA RICERCA

University of Parma Research Repository

Experimental study on the development of a micro-drilling cycle using ultrashort laser pulses

This is the peer reviewed version of the following article:

*Original*

Experimental study on the development of a micro-drilling cycle using ultrashort laser pulses / Romoli, Luca; Vallini, R.. - In: OPTICS AND LASERS IN ENGINEERING. - ISSN 0143-8166. - 78:(2016), pp. 121-131. [10.1016/j.optlaseng.2015.10.010]

*Availability:*

This version is available at: 11381/2815550 since: 2021-10-18T09:39:36Z

*Publisher:*

Elsevier Ltd

*Published*

DOI:10.1016/j.optlaseng.2015.10.010

*Terms of use:*

Anyone can freely access the full text of works made available as "Open Access". Works made available

*Publisher copyright*

note finali coverpage

(Article begins on next page)

Manuscript Number: OLEN-D-15-00091R1

Title: EXPERIMENTAL STUDY ON THE DEVELOPMENT OF A MICRO-DRILLING CYCLE  
USING ULTRASHORT LASER PULSES

Article Type: Original Article

Keywords: laser; ablation; microdrilling; stainless steel

Corresponding Author: Dr. L. Romoli, Ph.D. in Mechanical Engineering

Corresponding Author's Institution: University of Parma

First Author: L. Romoli, Ph.D. in Mechanical Engineering

Order of Authors: L. Romoli, Ph.D. in Mechanical Engineering; R. Vallini

**Abstract:** Microholes for the production of high precision devices were obtained by ultrashort pulsed laser machining of martensitic stainless steels. A micro-drilling cycle based on the sequence of a drilling through phase, an enlargement and finishing phase is proposed in order to solve the trade-off between process time and quality of the ablated surfaces without making use of complex design of experiments. The three phases were studied taking into account the evolution of the microhole shape as a function of the main process parameters (number of passes per phase, incidence angle and radius of the beam trajectory respect to the hole's axis).

Experiments testified that the drilling strategy was able to produce cylindrical holes with diameter of  $180 \pm 2 \mu\text{m}$  on a  $350\mu\text{m}$  thick plate in total absence of burrs and debris within a drilling time of 3.75 s.

Repeatability tests showed a process capability of nearly 99%.

SEM inspection of the inner surface of the microholes showed the presence of elongated and periodic ripples whose size and inclination can be controlled adjusting the incidence angle of the beam over the tapered surface before the ultimate finishing phase.



**UNIVERSITY OF PARMA**  
**IED - Industrial Engineering Department**  
**Parco Area delle Scienze 181/A, 43124 Parma - Italy**

Parma, 27 August 2015

**To: Dr. Pramod Rastogi**  
Editor, Optics and Lasers in Engineering

**Subject: Submission of a revised manuscript**

Dear Sir,

attached is the new version of the article entitled "EXPERIMENTAL STUDY ON THE DEVELOPMENT OF A MICRO-DRILLING CYCLE USING ULTRASHORT LASER PULSES". The revised manuscript has been prepared in accordance with the reviewers' valuable comments and suggestions.

I affirm that the manuscript has been prepared in accordance with Instructions to Authors. I have read the manuscript and I hereby affirm that the content of this manuscript or a major portion thereof has not been published in a refereed journal, and it is not being submitted for publication elsewhere.

Thank you very much.

Sincerely yours

Dr. Luca Romoli

A handwritten signature in blue ink, appearing to read "L. Romoli".

Complete address : Dr. ing. Luca Romoli  
Università di Parma  
Dipartimento di Ingegneria Industriale  
Parco Area delle Scienze 181/A  
43124 PARMA - ITALY  
phone: (+39)-0521-906202 (direct)  
e-mail: luca.romoli@unipr.it

We would like for first to thank the reviewers for the constructive comments. We have accepted and duly considered them all, as detailed in the following answers. We have produced a new version of the manuscript accordingly (for sake of simplicity we report in red in the text the changes made). Thanks to the reviewers' comments, we believe that the scientific content and the clarity of the present version are greatly improved.

**REVIEWERS' COMMENT:**

---

**REVIEWER #1:**

**The authors described very well a novel strategy for a high productive helical drilling process. Especially the use of the third phase to adjust not only the hole geometry but also the inner surface of the holes is innovative. The scientific quality is good, the authors described in detail the experiments and the used parameters. The experimental setup and the used methodology is reproducible for other scientist and appropriate to investigate the described problem. Only the description of the theoretical background needs some adjustments as described below. The paper fits very well to the field of this journal. The overall structure of the paper is clear and there are only minor changes and a more detailed description of the process capability necessary to accept the paper.**

---

1. "...Drilling high aspect ratio microholes in..."

**Definition of aspect ratio needed in section 1 instead of paragraph 1.1**

**Quantification of "high" aspect ratio is not really defined; in this study aspect ratio is in the range of 2. Is this really "high"? Definition needed.**

---

The reviewer is right in pointing out that the term "high" sounds qualitative without a value of comparison. In our experience a challenge for laser microdrilling is to produce cylindrical holes whose thickness is larger than the hole diameter in a reasonable industrial cycle time. The text was amended according to this concept.

---

2. "...This is because the electrical discharge produces very high temperatures at the point of the spark on the surface of the specimen, removing material by melting and vaporization. Thus, this process causes a ridged surface whose extremely rapid cooling may induce micro-cracks due to the high tensile residual stresses."

**Correction needed: This argumentation is also valid for machining with USP (ultra short pulsed) laser, in this case the process temperature is also above evaporation temperature and with extremely rapid cooling. The difference between machining with USP (ultra short pulsed) laser and micro EDM is not the temperature but the amount of heat remaining in the work piece.**

---

The sentence was corrected according to the reviewer's suggestion.

---

3. "...According to the literature [10], a pulse is ultrashort when the diffusion depth during the pulse is in the same order or smaller than the skin layer depth in the Beer-Lambert absorption law...."

This could be a definition for "ultrashort" but in this case the same laser could be "ultrashort" for one material and "only" short for processing another material. The common understanding is that USP lasers are below ns pulse duration. Suggestion for modification: "...According to [10]..."

---

---

instead of "...According to literature...".

---

The correction was implemented in the text.

---

4. "...With ultrashort laser pulses and high energy density the material is removed by cold ablation:..."

**Especially for metals the deposited energy is transferred from electrons to the lattice via electron-phonon coupling and the material is heated (very rapidly) up. This is in the most cases no "cold" ablation. Additionally all energy below the ablation threshold according to the Beer-Lambert law remains in the material as heat. Suggestion for modification: "...removed with minimized heat impact..." instead of "...cold ablation..."**

---

The correction was implemented in the text.

---

5. "...The effect of pulse duration on the HAZ can be explained by comparing the pulse duration  $t_i$  with the electron relaxation/cooling time  $t_{el}$  (in the order of 1 ps) and the time for electron to transfer energy to lattice  $t_{ion}$  (lattice heating time).  $t_{el}$  and  $t_{ion}$  are proportional to the heat capacity, and having electrons a much smaller heat capacity than the lattice it results:  $t_{el} \ll t_{ion}$ . For pulses in the femtosecond range ( $t_i \ll t_{el} \ll t_{ion}$ ) the pulse duration is much shorter than the time required for electron to relax and transfer energy to the lattice. Electrons are excited instantly and in about 1 ps they transfer energy to the positive ions. If the pulse energy is high enough, ions excitation can break the lattice bonding. Direct solid-vapor transition occurs because of insufficient time to transfer energy to neighboring lattice ions. Heat conduction is thus negligible and HAZ minimal [7, 10]."

**Instead of the reference [10] it should be referred to [Chichkov, B. N., Momma, C., Nolte, S., Von Alvensleben, F., & Tünnermann, A. (1996). Femtosecond, picosecond and nanosecond laser ablation of solids. *Applied Physics A*, 63(2), 109-115.] this is the reference for the description in [10] and possible also for [7].**

---

We would like to thank the reviewer for this correction. The missing reference was obviously a mistake from our side.

---

6. "...The literature testifies that a concrete method to control process parameters in the laser drilling of microholes is up to now not available or difficult to be applied to control mass production and predict output quality responses. ..."

**There are several publications describing methods for high quality laser drilled holes like [Kraus, M., Collmer, S., Sommer, S., & Dausinger, F. (2008). Microdrilling in steel with frequency-doubled ultrashort pulsed laser radiation. *J. Laser Micro/Nanoengineering*, 3(3), 129-134. ] additional there are several companies who do laser drilling especially of injection nozzles. Suggestion for modification: Skip the sentence.**

---

The sentence was deleted in the revised manuscript.

---

---

7. "...and ground up to the selected thickness..."  
**...grinded...**

---

The correction was implemented in the text.

---

8. "...Single pulse drilling is mainly used in small thickness parts or holes with less than 0.1 aspect ratios..."

**Reference needed for single pulse drilling, [15] describes only percussion drilling**

---

The missing reference was added in the revised manuscript.

---

9. "...the center of rotation (positioned at the intersection between the axis of the beam and the axis of the hole) can be set above or under the specimen. During the tests the first configuration was used..."

**Quantification of this value needed, where is the center of rotation located in respect to e.g. the focal position.**

---

The precession unit inside the scanning head allows to set the center of rotation above or under the specimen by the displacement of two optical wedges. The position of the center of rotation can be located at a distance of  $\pm 60$  mm from the focal plane which corresponds to the focal length of the adopted telescopic lens. If the center of rotation is positioned above the specimen the incidence angle results in positive values while for negative values the center of rotation is located under the specimen.

This information is now reported in the revised manuscript.

---

10. "...The graph of the conical factor (CF) indicates that it is possible to reduce the taper significantly increasing the number of passes, irrespective to the incidence angle adopted in the enlargement phase..."

**Please refer to Fig.7**

---

The missing reference was implemented in the text.

---

11. Section 3.4

"...produce cylindrical micro-holes even though configuration 3 has a process capability in the obtainment of CF of only 56%..."

**What was the method to calculate the process capability? Please describe in detail or refer to the used method.**

---

The process capability was calculated as the ratio between the required tolerance field ( $\pm 2$   $\mu\text{m}$  with respect to the average value of 180  $\mu\text{m}$ ) and the tolerance obtained after the drilling process

---

---

for the six sets of process parameters. Being 178  $\mu\text{m}$  and 182  $\mu\text{m}$  the lowest and the highest limits respectively, we standardized these limits according to the variance obtainable with a certain set of parameters and we considered the number of events falling outside these boundaries as a percentage of the 30 holes performed. The result is the process capabilities of the three events:  $D_{\text{in}}$ ,  $D_{\text{out}}$  and CF.

This concept is now reported in the section 3.4.

---

**12.** Fig. 3 "Influence of the incidence angle on the material removal in: (a) drilling of the pilot hole, (b) enlarging and finishing phases."

**The difference between (a) and (b) is not clear from the picture, the beam in case (a) should end at the surface of the material to make it clear.**

---

The correction was implemented in the figure.

---

**13.** Fig.5-Fig.8

**Please use a larger x-axis, the first and the last results should not be on the y-axis / border of the graph.**

---

The correction was implemented in the figures 5 and 6 in which the error bars were hidden by the borders of the graphs.

---

**14.** Fig. 7 and 8:

**The CF is unitless not (a.u.)**

---

The correction was implemented in the figures.

---

**15. In section 1, following reference should be added as mentioned above:**

Chichkov, B. N., Momma, C., Nolte, S., Von Alvensleben, F., & Tünnermann, A. (1996). Femtosecond, picosecond and nanosecond laser ablation of solids. Applied Physics A, 63(2), 109-115.

---

The reference was introduced as suggested by the reviewer.

---

**REVIEWER #2:**

**The paper deals with an experimental study of the microdrilling process with ultrashort laser pulses of a steel target for automotive applications.**

**The work is primarily focused on the technological purpose to find a trade-off between quality and time for the production of a well defined micro-hole geometry on a material of specific interest with a high degree of process reliability. With this scope, the best laser process strategy is investigated.**

---

---

Therefore, the technical and scientific content of the paper does not add anything new to what already known and present in the literature on the ultrafast laser microdrilling process itself, although it might be relevant from an application point of view but it .  
Nonetheless, the paper is well written and organized and could be considered for publication after suitable mandatory revisions.

---

**1. Page 2, section 1.1: The authors assert that**

"if it is worked close or under the ablation threshold, ultrashort laser pulses allow for refined material removal and nearly melt-free ablation".

**This is not completely true, because if the laser fluence is below the ablation threshold then no material removal would take place. In any case in this section describing the different ablation regimes depending on the incident fluence, the authors should better cite the paper from Nolte et al. "Ablation of metals by ultrashort laser pulses" J. Opt. Soc. Am. B, 14(10) 2716-2722 (1997).**

---

The sentence was corrected according to the reviewer suggestion.

A basic reference on the preliminary work of Nolte and his coauthors was included, as also requested from reviewer#1.

---

**2. Page 3, section 1.2: The authors should better specify and provide adequate references for the following sentence:**

"The literature shows that shortening the pulse duration under the photon-phonon relaxation time is not enough to provide an excellent quality of the ablated hole. The drilling strategy is also fundamental to avoid thermal affection to the workpiece ...".

**In particular, shortening the pulse duration is always a good strategy to avoid thermal damage to the material but it is important to work in a "gentle" ablation regime with a near-threshold fluence (see previous reference) and with a moderate repetition rate to prevent heat cumulative effects. With this regards the authors should better cite the following two papers: Ancona et al. "High speed laser drilling of metals using a high repetition rate, high average power ultrafast fiber CPA system," Opt. Exp. 16, 8958-8968 (2008) and Ancona et al. "Femtosecond and picosecond laser drilling of metals at high repetition rates and average powers," Opt. Lett. 34, 3304-3306 (2009). Then, I agree that the drilling strategy is also important.**

---

The text was revised according to the correction provided by the reviewer and the two meaning references added to the list.

---

**3. Page 4, section 2.2: The authors claim that percussion drilling technique has a "lack of reproducibility due to the high presence of melt material ...". This is actually not completely true because when working with ultrashort pulses, relatively thin materials and near-threshold laser fluence together with moderate repetition rates, the hole is not affected by melting. As well as, it is not true that holes produced with laser trepanning have a "very poor quality ... due to the fact that multiple passes must be performed on the same circular track without giving the time to the material to cool down, even using ultrashort laser pulses" because high quality and melt-free holes have been demonstrated working at a near-threshold laser fluence and moderate repetition rates. The only real limit of these techniques is the uncontrollable taper.**

---



---

Both the statements were deleted from the revised manuscript. The text was revised taking into account the information provided by the reviewer.

---

**4. Page 5, section 2.2: for the sake of clarity the Rayleigh length depends on the focal lens length, beam quality and beam size impinging on the lens and not on the beam waist even though the beam waist depends on the aforementioned parameters. In any case the authors should better mention the Rayleigh length of their specific experimental study in order to check if it is of the same order of magnitude of the workpiece thickness. In addition more details are required to describe their experimental setup like the type of focusing lens they used with the scan-head (focal length, F-theta ?, Telecentric ?). Table 1 should not confuse laser specs with other parameters like rotational frequency and spot diameter if it is entitled "laser source characteristics".**

---

We acknowledge the reviewer for the clarification about the dependence of the Rayleigh length on the optics adopted. All the text was modified for sake of clarity as well as the value of the Rayleigh length.

The beam delivery system used for experiments is a customized precession scanning head from Arges. The scan head is located after the objective in the beam path: the curvature of the focal plane is compensated by a moving telescopic lens with a focal length of 60 mm.

A rough beam with a diameter of  $3.8 \pm 0.2$  mm is conveyed into the scanning head and then circularly polarized by a  $\lambda/4$  plate before entering the precession unit. The precession unit is constituted by two wedges whose misalignment determines the inclination of the beam with respect to the optical axis. This misalignment is controlled by the incidence angle set on the controlling software of the scanning head according to what already described in the manuscript. After the precession head the beam passes through a motorized focusing lens before reaching the X-Y galvo head.

In order to check the information reported above we recommend to refer to [http://www.arges.de/index.php?id=precession\\_elephant0](http://www.arges.de/index.php?id=precession_elephant0).

---

**5. In figure 2 the beam is represented perpendicular to the workpiece surface, which is actually not the case as explained in figure 3.**

---

The reviewer is right in pointing out this contradiction. In our idea figure 2 should only express the beam trajectories in the different phases since the incidence angle is introduced in the next paragraph. Nevertheless we understand that this can induce confusion into the reader. The beam trajectories are now deleted from figure 2.

---

**6. End of page 8, section 3.1: The authors claim that: "Laser trepanning on a radius of 20  $\mu$ m respect to the hole axis (fig. 4.b) resulted in uncompleted or irregular holes. The ablation left an internal core that was only in few holes indirectly ablated due to energy absorption. It was supposed that in most cases this internal core tilted and hindered the beam to penetrate through the specimen thickness." The authors should mention that by doubling the rotation radius a much higher number of passes than 90 is probably needed to breakthrough the workpiece thickness.**

---

---

We agree with the reviewer comment on the fact that the breakthrough of the specimen would have been possible using a number of passes higher than 90 but this would have brought to a not justified increase in the drilling time with respect to other alternatives.  
In any case, for sake of clarity, the text was modified accordingly to the comment above.

---

**7. Page 11, section 3.2: The authors claim that "The effect of the incidence angle on the dimension of the exit diameter is negligible at low number of passes". This is obvious because in the first passes most of the laser energy is employed to enlarge the input diameter, as seen in figure 5. Here, the incidence angle has a greater influence at low number of passes.**

---

We believe that the sentence is rather obvious, as the reviewer says, but not trivial since it clarifies to a possible industrial user how to control the effects of the incident angle parameter.  
The sentence was reworded to incorporate reviewer's suggestion.

---

**8. Figure 8. The authors should better explain and comment on the fact that for 250 number of passes and a higher incidence angle of  $2^\circ$ , the conical factor increases. Is there a physical explanation for this result ? Is it possible that in this last case also the input hole diameter was enlarged due to the higher incidence angle an number of passes thus justifying a CF value different from the expected trend ?**

---

The explanation of the phenomenon reported by the reviewer has been enriched in the revised manuscript following the concept detailed here below.

According to our measurements, 250 passes (but also more severe conditions were tried with 300 passes) performed with  $\theta_i=2^\circ$  did not produce an enlargement of the at the highest value outside of the allowed tolerance of  $\pm 2 \mu\text{m}$ . Conversely, finishing phases with  $\theta_i>2^\circ$  showed always a restriction of the exit diameter with deposition of melt materials or even burrs. Our explanation to this phenomenon is that increasing (even slightly)  $\theta_i$  reduces the angle with which the beam impinges of the conical inner surface generated by the enlargement phase. In these conditions more energy can be transferred to the material inside the microhole which results in the formation of melt material closing the exit diameter or hindering the beam to reach a complete ablation of  $D_{\text{out}}$ .

As a result there's a trade off in the use of  $\theta_i$ : a sufficient value is needed in order to obtain a cylindrical shape of the hole in the minimum drilling time but increasing its value determines an increase in the energy transferred to the workpiece. This means that (for the hole geometry under consideration) the number of passes should not be increased at the same time in order to avoid the formation of burrs.

Then we agree with the reviewer: a further increase in the use of  $\theta_i$  may lead to an unwanted contact of the beam with the opposite (phase shift of  $180^\circ$ ) side of the hole with a further and uncontrollable increase of the inlet diameter. This phenomenon was underlined in the conclusions.

---

**9. Finally, a comment of the authors would be appreciated on the following claim: "The hole taper can be then retained the main responsible of the elongation and orientation of the ripples." In which way the hole taper affects the ripple orientation along the hole ? Considering that the hole taper changes during the different drilling steps, how does this affect the ripple orientation ? Is the ripples orientation homogeneous along the hole depth ? In fact, a different intensity distribution and different incident angle of the laser radiation on the hole internal**

---

---

**wall is expected at different hole depths.**

---

According to Reif et al. (see reference below), the strong correlation between polarization direction and ripples orientation suggests the absorbed electromagnetic field vector into the sidewall to be the main control parameter for the self-arrangement of the surface “soft” state induced by the laser on the inner wall. Elliptical polarization at normal incidence ( $\theta_i=0^\circ$ ) generates LIPSS elongated perpendicularly to the direction of the strong field (major axis of the ellipse).

Conversely, circular polarization (as the one used for experiments) does not lead to elongated LIPSS formation unless large  $\theta_i$  are used. This is because the strong anisotropy in absorption of the p- and s- light components at grazing incidence produces an anisotropy in the electromagnetic field absorbed by the material.

According to our experience performing the pilot hole is really far from the case of a ‘gentle ablation’ and a small plasma plume is often visible during this phase. Nevertheless the surface asperities generated in passing through the material may have an effect in the orientation of periodic pattern in the following phases. The enlargement phase is characterized by ripples on the conical inner surface which are in turn destroyed and rearranged in the finishing phase. Our assumption of considering LIPSS to evolve only in the last finishing phase is not so far from reality, as already testified in a previous research.

Concerning the last question, we thank the reviewer for having pointed out a relevant aspect. LIPSS inclination is not homogeneous along the hole depth. Our measurement revealed a maximum variation of about  $5^\circ$  from top to bottom. As the reviewer was foreseeing, this phenomenon depends on the different intensity distribution and different incident angle of the laser radiation on the hole internal wall at different hole depths.

J. Reif, O. Varlamova, F. Costache (2008) Femtosecond laser induced nanostructure formation: self-organization control parameters, *Applied Physics A* 92 pp. 1019–1024.

---

The entire part was revised in order to make this section more understandable for readers.

---

- ✓ Laser microdrilling can be analyzed as a conventional manufacturing process.
- ✓ Trade-off between quality and time is solved using a three step cycle.
- ✓ The evolution of the hole shape is linked to process parameters.
- ✓ Cylindrical microholes are achieved in absence of burrs and debris.
- ✓ Periodic ripples characterize the inner surface of the hole.

# EXPERIMENTAL STUDY ON THE DEVELOPMENT OF A MICRO-DRILLING CYCLE USING ULTRASHORT LASER PULSES

L.Romoli<sup>1</sup>, R.Vallini<sup>2</sup>

<sup>1</sup> Department of Industrial Engineering, University of Parma, Italy

<sup>2</sup> Department of Industrial and Civil Engineering, University of Pisa, Italy

## 1. Introduction

Drilling microholes in several materials has become one of the most interesting challenges for precision engineering during the last decade especially if the drilled thickness is larger than the microhole diameter. This is due to the very wide range of applications in which microholes have to be performed, starting from the biomedical sector to the automotive and aerospace industries. Surgical tools like ophtalmic needles are microdrilled with Electro-chemical Machining (ECM) or by electroerosion [1]. Cooling channels for turbine blades [2] or turbomachinery components [3] are often obtained with the same technologies. An even wider technical application is represented by the production of fuel injector nozzles. Cavitating nozzles for GDI engines are conventionally produced by micro-electrical discharge drilling with holes diameters between 150-200  $\mu\text{m}$  and thickness of about 250-350  $\mu\text{m}$ . This is a well tested technology which has proven to be reliable, however many limitations exist with regard to flexibility and surface quality [4]. According to the literature [5], micro-EDM with low pulse energies enables a minimum  $R_a$  of 0.3  $\mu\text{m}$ . This is because despite to the relative small discharge energies (generally ranging between 3 to 15  $\mu\text{J}$ ) the spark duration of about 60-100 ns transfers a significant amount of heat to the workpiece which is removed by melting and vaporization. Thus, this process causes a ridged surface whose extremely rapid cooling may induce micro-cracks due to the high tensile residual stresses.

Since the functionality of a microhole strongly depends on the diameter stability but on micro-geometrical details as well (e.g. surface roughness, inlet chamfer radius, presence of burrs, etc.), laser technology has recently demonstrated to be an alternative technique enabling to work in dry environment with an even higher flexibility in changing the hole design. Smoother internal surfaces can be achieved in shorter processing times by fs-laser ablation respect to micro-EDM [6]. The sharpness of the machined edges combined with a smooth surface can exploit best performances in terms of fluid-dynamics passing through the microhole.

### 1.1 Timescale reduction in pulsed laser machining

Thanks to last decades developments, laser drilling process has become an industrial solution for massive micro or small holes drilling, ranging hole diameters from 5 $\mu\text{m}$  to 1mm, aspect ratios (ratio between drilled thickness and hole diameter) higher than one and wide range of work piece materials. The combination of pulse peak power and duration significantly influences the material removal mechanism. For long pulses (micro- and nano-second) and low energy density, the material is removed by melt expulsion, combining material vaporization and melting. Those sources show high production rates against low quality generated by melt accretions and thermal damage of the workpiece [7-8]. Due to the large amount of melt ejection and spatter formation involved in the process, the quality and reproducibility of the hole is rather low [9].

If higher precision is needed, short and ultrashort laser pulses have to be applied. According to [10], a pulse is ultrashort when the diffusion depth during the pulse is in the same order or smaller than the skin layer depth in the Beer-Lambert absorption law. With ultrashort laser pulses and high energy density the material is removed with minimized heat impact: the laser interacts with the material in the solid state only, and direct solid-vapor transition occurs. In case of metals, 1 ps can be retained a threshold value for transition from short to ultrashort [7].

Ultrashort laser pulses achieve higher quality removal processes with a nearly negligible heat affected zone (HAZ). The effect of pulse duration on the HAZ can be explained by comparing the pulse duration  $t_i$  with the electron relaxation/cooling time  $t_{el}$  (in the order of 1 ps) and the time for electron to transfer energy to lattice  $t_{ion}$  (lattice heating time).  $t_{el}$  and  $t_{ion}$  are proportional to the heat capacity, and having electrons a much smaller heat capacity than the lattice it results:  $t_{el} \ll t_{ion}$ .

For pulses in the femtosecond range ( $t_i \ll t_{el} \ll t_{ion}$ ) the pulse duration is much shorter than the time required for electron to relax and transfer energy to the lattice. Electrons are excited instantly and in about 1 ps they transfer energy to the positive ions. If the pulse energy is high enough, ions excitation can break the lattice bonding. Direct solid-vapor transition occurs because of insufficient time to transfer energy to neighboring lattice ions. Heat conduction is thus negligible and HAZ minimal [11]. Therefore, if it is worked close to the ablation threshold, ultrashort laser pulses allow for refined material removal and nearly melt-free ablation. A direct output of the above exposed physical phenomena can be traced back to authors' previous experience in [6] concerning the surface roughness obtainable with such process. Ultrashort pulses ablation has demonstrated to produce holes with inner surface roughness lower than 100 nm ( $R_a$ ) compared to those obtained with micro-EDM ( $R_a=300-400$  nm). Besides, the cutting edges obtained with ultrashort laser pulses are sharper (radius 0.6 - 0.8  $\mu\text{m}$ ) compared to  $\mu$ -EDM ones (radius 3 - 4  $\mu\text{m}$ ).

These peculiarities promote the industrial application of fs-laser sources for the mass production of microholes under the limitation of aspect ratios obtainable with a single focusing procedure. Nevertheless, a production drilling machine based on fs-laser ablation requires the development of a drilling strategy which can maximize the removal rate maintaining the very high quality of the hole described above. The technique by which the laser is moved over the specimen to create a cylindrical hole is a keyfactor for an optimized use of these laser sources as well as a selection of process parameters. The optimization of this strategy has to be performed as a trade-off among multiple objectives which should be fulfilled simultaneously (e.g. quality, drilling time, energy consumption, etc.). Attempts in this sense have been done in [12] using the Taguchi's method: this method originally designed to optimize a solitary quality characteristic, was also tested in case of multi-response optimization for high-quality microdrilling on plastics. Taguchi's design of experiments was also used in [13] to study the effects of the process variables on the quality of the drilled holes: minimum taper in the drilled hole was considered as the desired target response. A central composite design (CCD) based on response surface methodology (RSM) was employed in [14] for multi-objective optimization of pulsed Nd:YAG laser microdrilling operations on gamma-titanium aluminide alloy. The knowledge of the effect of laser related process variables on hole related responses with respect to variation of sample thickness was found essential to obtain a hole of required quality. Therefore, in [15] a coupled methodology

comprising of Finite Element Method (FEM) and Artificial Neural Network (ANN) was used to develop a prediction model for the laser beam percussion drilling on nickel based superalloy.

## 1.2 Research objectives

This research aims at investigating the capabilities of a drilling technique based on femtosecond laser ablation for the industrial production of microholes in stainless steels similar to those adopted for automotive applications. As a consequence cylindrical holes of  $180 \pm 2 \mu\text{m}$  of diameter have to be obtained on a  $350 \mu\text{m}$  thick plate (while the common thickness for fuel nozzles is up to now of  $250 \mu\text{m}$  [4]) in the lowest cycle time possible with the required reproducibility and quality. The main objectives of the experimental activity can be pinpointed as follows.

- Tests were designed to assess the feasibility of a drilling cycle enabling the cylindrical shape of the hole and the shortest cycle time, as well. The dependence of the microhole geometrical features (e.g. diameter, taper angle, burrs, surface appearance) on process parameters has to be preliminary identified and understood.
- The literature shows that shortening the pulse duration **is always a good strategy to avoid thermal damage to the material but it is important to work in a ‘gentle’ ablation regime with a near-threshold fluence [11] and with a moderate repetition rate to prevent heat cumulative effects as also underlined in [16] and [17] for the case of laser ultrashort pulse laser drilling. Nevertheless the drilling strategy is also fundamental to avoid thermal affection to the workpiece:** the objective is to subdivide microdrilling in sub-phases with the twofold objective of reducing the interaction time of the laser on the material and keeping the final shape cylindrical. For each step of the drilling cycle the dependence of the shape on process parameters has to be understood and studied in detail in order to define the guidelines for the optimization process.
- Final target of the experimental tests is to verify if the subdivision in drilling phases can accomplish the multiple design criteria for the hole characteristics (e.g. balancing a roughing phase and a finishing phase to obtain the finest quality in the shortest time), as in a conventional manufacturing operation.

## 2. Experimental details

### 2.1 Specimen design

The material selected for the experimental study is AISI 440C (pre-hardened and tempered). This stainless steel is commonly used in automotive industries for the fabrication of fuel injectors since it combines high hardness and good resistance to chemical corrosion. Arrays of holes obtained with different parameters combination are performed on a  $350 \mu\text{m}$  thick sample. The sample thickness selected corresponds to an aspect ratio (thickness/hole diameter) close to 2. Samples to be drilled are cut from a cylindrical bar and **grinded** up to the selected thickness.

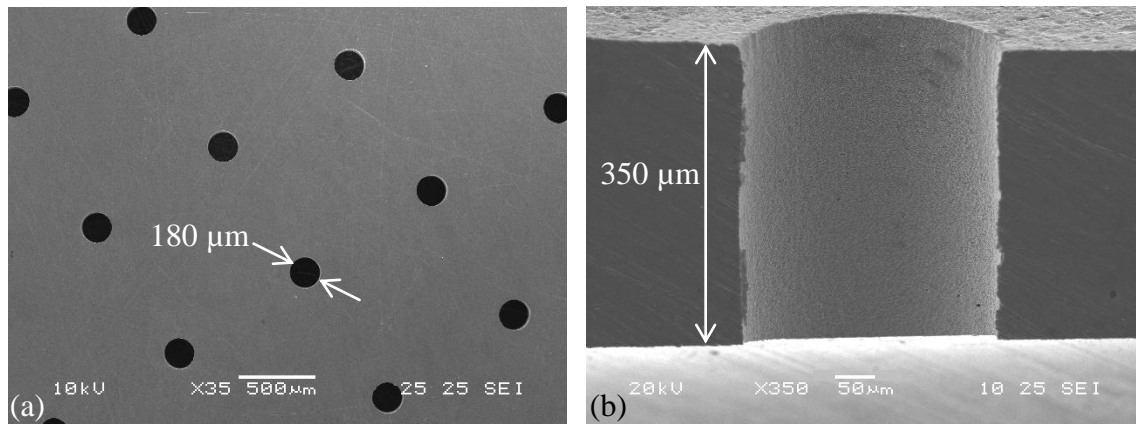


**Fig. 1** - (a) SEM view of a microholes matrix drilled on a specimens; (b) cross-section of a microhole: the top surface is the entry side on which the laser is focused.

## 2.2 Drilling techniques

Laser drilling techniques are divided in two categories: one performed with steady-beam, and the others obtained with the beam in motion. Both categories use pulsed laser sources. Single pulse laser drilling and percussion drilling belong to the first group. Single pulse drilling is mainly used in small thickness parts or holes with less than 0.1 aspect ratios. Laser percussion drilling is based on removing material by sequence of pulses: each pulse removes a certain volume of material so that the entire sequence of pulses can achieve deep hole size with diameters ranging between 25 and 500 μm. Both techniques are characterized by high productivity and rather reproducible results if **near-threshold laser fluence together with moderate repetition rates** are adopted to drill thin materials. On the other hand the hole taper is uncontrollable taper **as reported in [18] and [19]**.

Laser trepanning and helical drilling are included in the second category. In laser trepanning the beam moves in circular trajectories to cut the perimeter of the hole [20]. In helical drilling the laser beam rotates continuously at the nominal diameter shifting the focal position, so that the spot produces a helical trajectory inside the material [21]. These techniques guarantee better circularity respect to those with steady-beam and **high quality and melt-free holes have been demonstrated working at a near-threshold laser fluence and moderate repetition rates. Nevertheless the fact that multiple passes must be performed on the same circular track does not allow to control the taper and to obtain cylindrical holes [22]**.

The technique here developed differs from those reported in literature since it is composed by a refined material removal based on the three following steps also depicted in fig.2. Each phase fulfills an exact target to reach the expected shape in the shortest time as possible.

- **Pilot-hole:** during this first step a through hole of small diameter (40 – 60 μm) is created. This hole allows the ablated material to be expelled during the drilling process, in order to improve laser-material interaction. The pilot hole allows the beam to interact on the whole thickness of the sample during the next phase avoiding thermal affection conversely to conventional trepanning. The pilot-hole can be created both rotating the beam at constant radius (respect to the axis of the hole) and moving it in spiral from the axis of the hole to a definite radius.



- **Enlargement:** during this second phase the beam rotates from the pilot-hole radius up to the nominal radius, in a spiral trajectory. The spiral has a radial increment per turn depending on the number of passes of the corresponding phase. At the end of the enlargement phase the hole is expected to have a significant taper ( $D_{in} \geq D_{out}$  with respect to the direction of the beam). The intent of this roughing phase is to maximize the removal rate without considering hole taper and surface quality.
- **Finishing:** a last phase is hypothesized to achieve a cylindrical geometry with a refined quality. In this phase the beam rotates at nominal diameter for a sufficient number of passes to remove the material left by previous phase at the exit side of the hole. The beam smoothens the surface bringing the inner wall to an uniform surface roughness, as in [6].

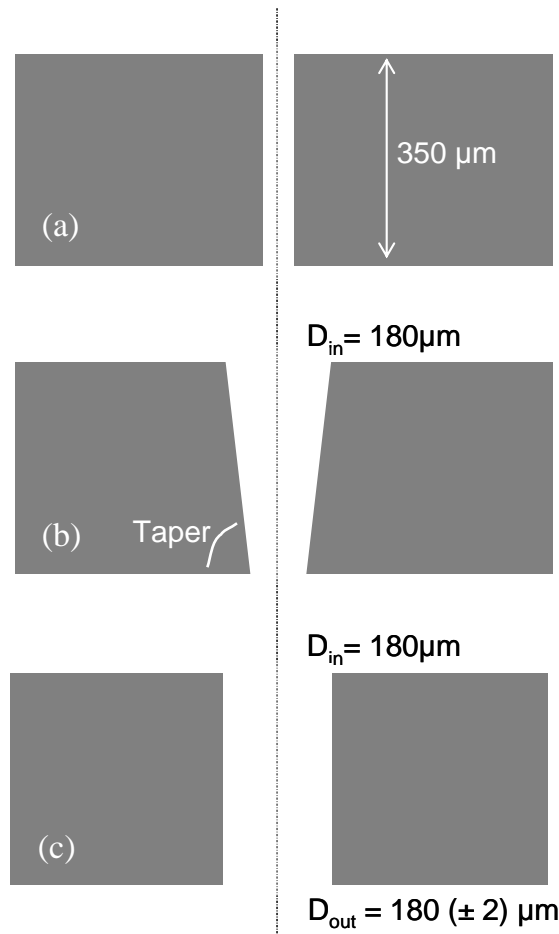


**Fig. 2** – Drilling steps from top to bottom: (a) drilling through phase or pilot-hole, (b) enlargement phase and (c) finishing phase.

Using a 60 mm focal length lens, the Rayleigh length for the adopted laser set-up is nearly  $300 \mu\text{m}$ . This allows to perform the drilling process without moving the focal position. As a consequence the focal position of the beam remains on the surface of the specimen during the whole process. This drilling technique based on sequential phases is designed to produce high quality holes, characterized by excellent circularity and cleanliness, which are fundamentals for the fluid-dynamics inside the nozzle. The three steps should limit the typical taper of laser drilled holes caused by the divergence of the beam and the different laser-material interaction with increasing depth.

### 2.3 Experimental set-up

The laser drilling machine used for experiments is a lab apparatus equipped with a Rofin (Ge) starfemto R-100 femtosecond fiber laser (details in table 1) which conveys a 3.8 mm unfocussed beam in an Arges (Ge) scanning head. The scanning head enables to set position, focusing and inclination of the beam giving it a precessional movement around the hole axis. The rough beam is circularly polarized by a  $\lambda/4$  plate before entering the precession unit. The precession unit is constituted by two wedges whose misalignment determines the inclination of the beam with respect to the optical axis. This misalignment inclines the beam with respect to the optical axis and can be adjusted as a control parameter of the process. After the precession head the beam passes through a motorized focusing lens (60mm focal length) before reaching the X-Y galvo head. Pressurized helium (0.7 MPa) was used as processing gas.

Wavelength [nm]	1552
Pulse duration [fs]	800
Spot diameter [ $\mu\text{m}$ ]	20
Pulse energy [ $\mu\text{J}$ ]	max 50
Pulse frequency [kHz]	max 100
Rotational frequency [Hz]	max 100

Table 1 - Laser source and beam delivery characteristics

Drilling parameters can be divided in two categories: one belonging to the laser source (pulse energy and repetition rate) the other to the scanning head (rotational frequency, number of passes per phase, incidence angle and radius of rotation respect to the hole's axis).

Due to the long setup times needed to stabilize the laser source, pulse energy and pulse frequency cannot be varied between two phases of the drilling process which normally last fractions of a second.

The rotational frequency expresses the maximum number of turns obtainable in 1 s by the scanning head. The reciprocal of the rotational frequency is the minimum obtainable time to perform a turn (e.g. 0.01 s at 100Hz): this minimum time is kept constant during one phase meaning that for spiral movements the travelling speed of the beam, tangential to the trajectory, increases linearly with increasing the spiral radius. The maximum tangential speed in the present study is about 50 mm/s reached at the trajectory radius of 80  $\mu\text{m}$  (considering the offset to the nominal diameter of the hole represented by the laser spot diameter).

Pulse energy, repetition rate and rotational frequency were set on maximum levels during the test, in order to maximize the ablation rate. In addition, the laser source was found to be more stable at the highest energy level and pulse repetition.

The incidence angle  $\theta_i$  represents the inclination of the beam axis respect to a line perpendicular to the material surface: the evaluation of the incidence angle varies if the beam is acting on a flat surface (fig. 3.a) or on a conical surface (fig. 3.b). In the first case, the scanning head allows a maximum  $\theta_i$  of about  $7^\circ$  allowing for a precessional movement: the center of rotation (positioned at the intersection between the axis of the beam and the axis of the hole) can be located at 60 mm above or under the specimen.

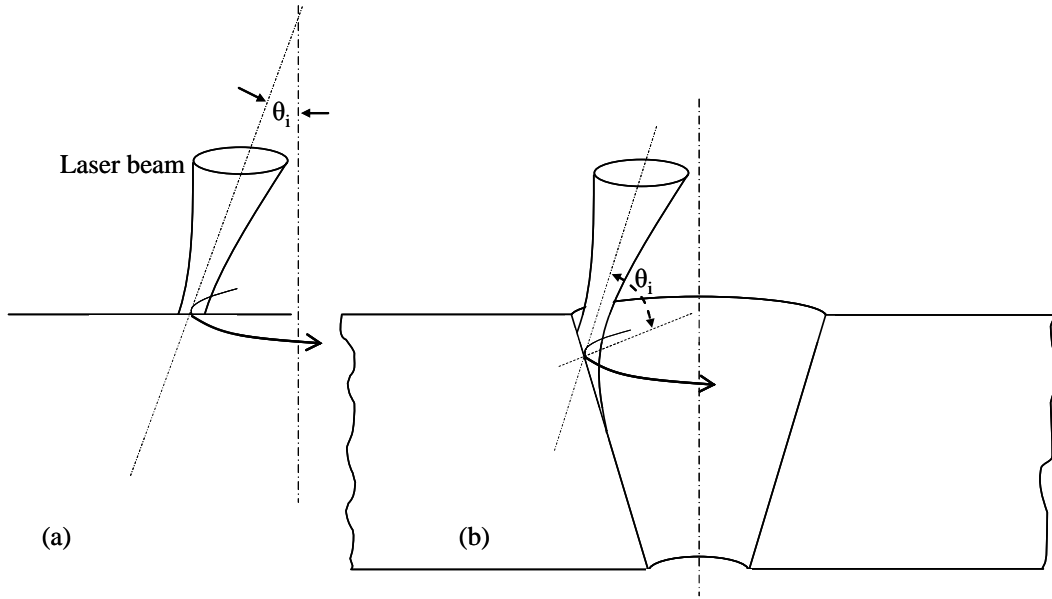


**Fig. 3** – Influence of the incidence angle on the material removal in: (a) drilling of the pilot hole, (b) enlarging and finishing phases.

During the tests the first configuration was used in order to recover to the natural taper of the microhole, deriving from the loss of energy at the increase of the drilling depth, without enlarging the entry side diameter of the hole. The drilling strategy developed in the present research is based on the hypothesis that inclining the laser beam during the enlargement phase should allow for a higher ablation rate by deploying the intense peak power of the fs-laser over a large irradiation area (as depicted in fig. 3 b). Conversely, the finishing phase should guarantee a refined ablation of the exit edge of the hole by a selective removal of the taper without thermally affecting the entry side.

The number of passes per phase, the incidence angle and the radius of rotation were varied during the tests, in order to verify the influence of these parameters on the hole characteristics. For each combination of parameters five holes were produced in order to assess the repeatability of the obtained results. After drilling, the specimen was washed in ultrasonic rinse of citric acid at 35° C to dilute residuals of burst at the entry and exit side of the laser. A proper cleanliness of the ablated surfaces allowed for the measurements of the of the entrance/exit diameters of the microhole under an optical microscope (quickscope – Mitutoyo) with a resolution of 0.1 μm. The measurements were done by illuminating the hole from the rear side and using a computerized vision system to identify series of points on the perimeter of the hole.

The diameters were measured three times each, and then arithmetically averaged. Starting from the entrance and the exit diameters, the taper (or Conicity Factor, CF) was calculated by means of the following equation:

$$CF = \frac{D_{in} - D_{out}}{L} \cdot 100 \quad (1)$$

where  $D_{in}$  is the inlet diameter and  $D_{out}$  the exit diameter respect to the beam direction,  $L$  is the thickness of the specimen (350μm).

As final inspection of the drilled microholes, cross-sections of the specimens were performed with a rotating grinder and analyzed with Scanning Electron Microscopy. The inner wall structures were determined and analyzed to ensure the stability of the drilling technique.

### 3. Results and discussion

The aim of the tests was to produce cylindrical holes of  $180 \pm 2 \mu\text{m}$  of diameter on  $350\mu\text{m}$  thick plate, studying the drilling parameters effects in each phase of the process in order to minimize the cycle time. The process should avoid debris and burrs at the edges, as well.

Taking into account that the drilling method is composed by three successive phases, it is hard to define a test layout according to the well-known experiments design criteria. The enlargement phase depends on how the pilot hole is realized, on its taper and especially on the possibility to have a proper evacuation of metal vapors through the specimen thickness. Similarly, the finishing is linked to the taper obtained in the enlargement phase: the higher the taper, the longer the time for the finishing phase to bring the microhole to the cylindrical shape. As a matter of fact the three phases are interdependent, being the output of the first one the boundary condition to start the next. As in a conventional manufacturing process based on the succession of multiple phases in a route sheet, finding the optimal condition to minimize the cycle time and to respect the design constraints of geometry and quality, has multiple solutions. The approach followed in this research, is based on empirical observations with the aim of investigating the influence of process parameters on the drilling time and the hole quality.

#### 3.1 Pilot-hole

Five holes for each combination of parameters listed in table 2 were executed (100 combinations).

Parameters	Values				
Radius of rotation [ $\mu\text{m}$ ]	Spiral $0 \rightarrow 10$	Spiral $0 \rightarrow 20$	Constant 10	Constant 20	
Number of passes	30	45	60	75	90
Incidence angle [ $^\circ$ ]	0	1.5	3	4.5	6

Table 2 – Pilot-hole drilling parameters. The spiral has a radius increment per turn depending on the number of passes of the phase.

A first observation under the microscope of the performed pilot holes showed the following evidences:

- High incidence angles ( $6^\circ$ ) produce holes with non-circular exit edge. This is because for drillings with a high aspect ratio as the pilot hole (about 6), reflections at the hole inner wall take place, leading to a non-uniform intensity distribution deep inside the formed hole as also reported in [23].
- 30 passes are not enough to obtain a through hole;
- Several holes obtained using a spiral trajectory from hole's axis ( $r=0 \mu\text{m}$ ) to radius  $10\mu\text{m}$  did not pass through the workpiece. This defect can be traced back to the delay in laser activation for such small trajectories. Moreover deposits could be found at the exit.

Then the diameters of the holes were measured and the CF factors evaluated. With the aim of verifying the effect of the pilot-hole taper on the enlargement phase, three sets of parameters were selected among the whole set of data which ensure CF of  $(-5; 0; +5)$  respectively, in the lowest time as possible. The parameters are listed in table 3. The drilling time can be calculated dividing the number of passes by the rotational frequency, 100 Hz.

	CF ~ -5	CF ~ 0	CF ~ +5
Radius of rotation [ $\mu\text{m}$ ]	Constant 10 $\mu\text{m}$	Constant 10 $\mu\text{m}$	Constant 10 $\mu\text{m}$
Incidence angle [ $^\circ$ ]	4.5	3	0
Number of passes	75	60	45
Phase time [s]	0.75	0.60	0.45
Averaged $D_{\text{in}}$ [ $\mu\text{m}$ ]	40.75	39.55	37.10
Averaged $D_{\text{out}}$ [ $\mu\text{m}$ ]	57.55	41.25	20.20

Table 3 – Pilot-hole selected

It can be noticed from table 3 that the best results selected for further investigation in the enlargement phase were obtained by a conventional trepanning at the constant radius of 10  $\mu\text{m}$  respect to the hole axis (being the ellipticity of the spot almost negligible up to  $7^\circ$ ). This means that the focused spot is always tangent to the hole axis and the material is completely ablated as reported in the draft in fig. 4.a. The pilot hole diameter at the entry side is nearly 40 $\mu\text{m}$  for all the CF under consideration. This means that pure ablation is obtained, without any further removal due to energy conduction to the surroundings. Laser trepanning on a radius of 20 $\mu\text{m}$  respect to the hole axis (fig. 4.b) resulted in uncompleted or irregular holes. The ablation left an internal core that was only in few holes indirectly ablated due to energy absorption. It was supposed that in most cases this internal core tilted and hindered the beam to penetrate through the specimen thickness. **It should be noted that by doubling the rotation radius a much higher number of passes than 90 is probably needed to breakthrough the workpiece thickness: this would lead to a significant increase in the drilling time.**

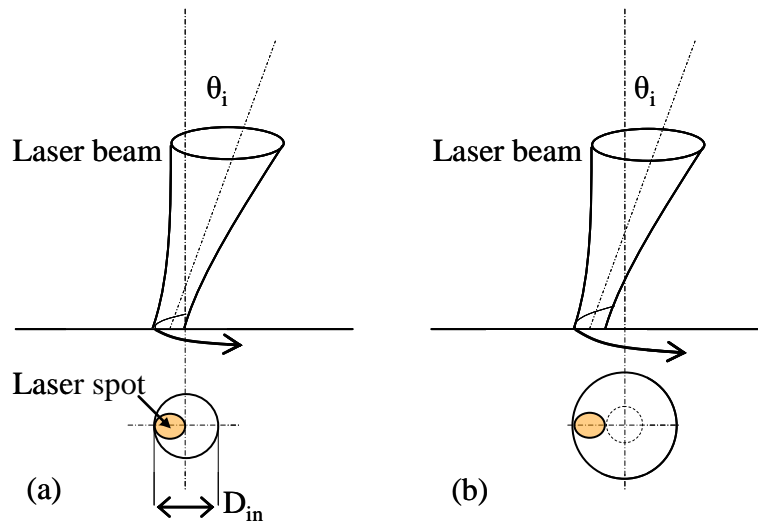


Fig. 4 – Drilling of the pilot hole using circular trepanning: (a) trajectory radius=10 $\mu\text{m}$ , (b) trajectory radius=20 $\mu\text{m}$ .

### 3.2 Enlargement

In the enlargement phase the beam carried out a micro-cutting operation more than a real drilling, since it removed the material on the entire thickness of the specimen along a trajectory starting from the pilot-hole radius up to the nominal hole radius. The pilot-holes selected in the previous phase were initially enlarged using the combination of parameters showed in table 4 (45 combinations). Increasing the number of passes results in a reduction of the radial increment of the spiral trajectory: 75 passes correspond to 0.95  $\mu\text{m}$  per turn of radial ablation, 200 passes correspond to 0.35  $\mu\text{m}$  per turn.

Parameters	Values				
Incidence angle [°]	0	1	2		
Number of passes	75	90	105	135	200

Table 4 – First enlargement attempt parameters

Measurements at the optical microscope showed the following results:

- A number of passes lower than 135 did not produce any significant enlargement of the exit diameter. The energy loss along the thickness of the material imposed a higher limit to the radial overlap between adjacent passes.
- Increasing the incidence angle resulted in higher exit diameter: this effect confirmed the hypothesis depicted in the sketch of figure 3.
- The holes enlarged starting from a negative tapered pilot-hole (CF~ -5) showed higher exit diameter. A negative taper offered better conditions for the evacuation of particles and metal vapors enabling a better absorption of laser energy.

According to these results, a second attempt was done using a negative tapered pilot-hole as boundary condition for the enlargement phase using higher number of passes and higher incidence angle respect to previous tests. Parameters utilized for the second enlargement attempt are showed in table 5.

Parameters	Values				
Incidence angle [°]	2	3	4		
Number of passes	150	175	200	250	300
Phase time [s]	1.5	1.75	2	2.5	3
Total time [s]	2.25	2.5	2.75	3.25	3.75

Table 5 - Second enlargement attempt parameters. Total time result the sum of the two phases (pilot-hole cycle time 0.75s).

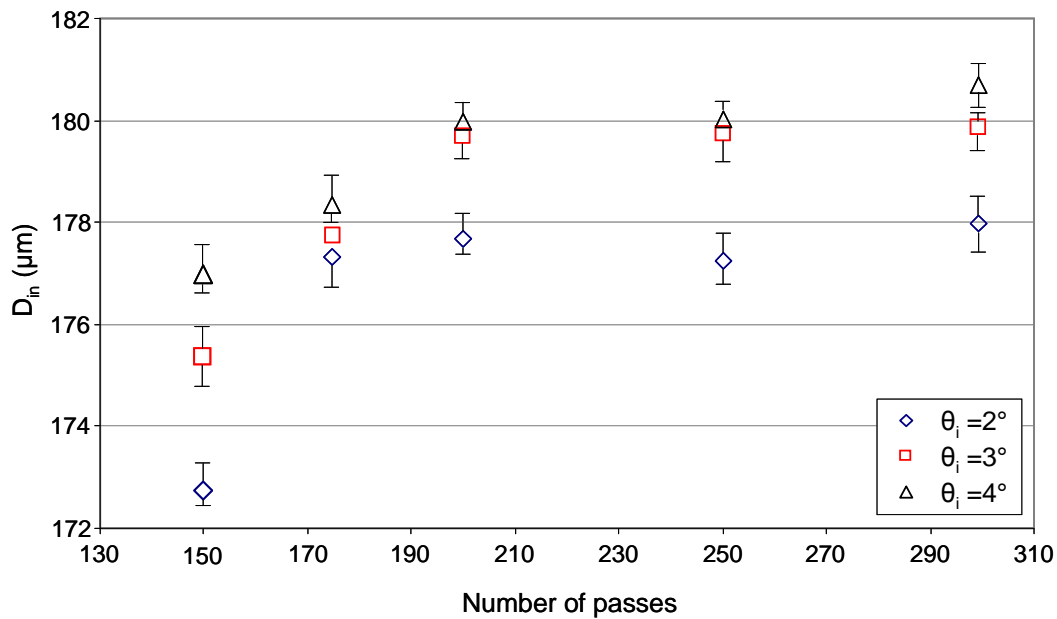
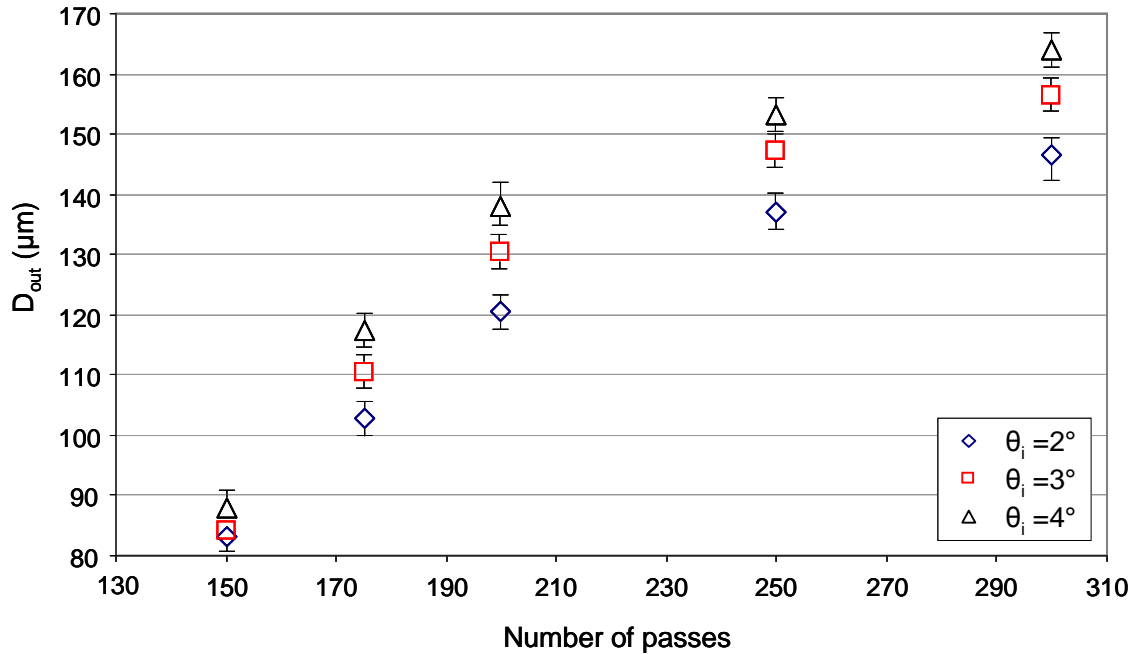


Fig. 5 - Inlet diameter variation in enlargement phase.

The results of the second set of experiments are summarized in the following graphs: each point represents the arithmetic mean value calculated on the five holes produced with the same parameters. The mean value of the experimental measurements is associated to the related data dispersion.

Figure 5 shows that the inlet diameter increases with the number of passes up to 200 passes. Beyond this value it remains near to the nominal value of 180  $\mu\text{m}$ : this means that further passes are useless but do not compromise the tolerance on the entry side diameter.

Conversely figure 6 shows that the exit side diameter grows with the number of passes, independently from the incidence angle. The reduction of the radial increment per turn (obtained by increasing the number of passes) produces larger outlet diameter: this is probably due to the fact that the beam has to ablate less material during the cutting trajectory and more energy is available at the exit side.



**Fig. 6** - Exit diameter variation in enlargement phase.

The effect of the incidence angle on the dimension of the exit diameter is obviously negligible at low number of passes: during the first passes most of the laser energy is employed to enlarge the inlet diameter. As the number of passes increases, higher incidence angle during enlargement produces larger outlet diameter, as already demonstrated for the pilot-hole phase. It can be noticed that figure 5 has a smaller scale on the y-axis respect to figure 6. This is intentionally done to magnify the data dispersion which demonstrates the higher repeatability of the entry side diameter respect to the exit side one.

As a result, none of the configuration tested above allows for the production of a cylindrical hole at the end of enlargement phase. The graph of the conical factor (CF) reported in figure 7 indicates that it is possible to reduce the taper significantly increasing the number of passes, irrespective to the incidence angle adopted in the enlargement phase. This reduction of CF is more pronounced up to 200 passes while for higher values the decrease is less pronounced, especially using high incidence angles.

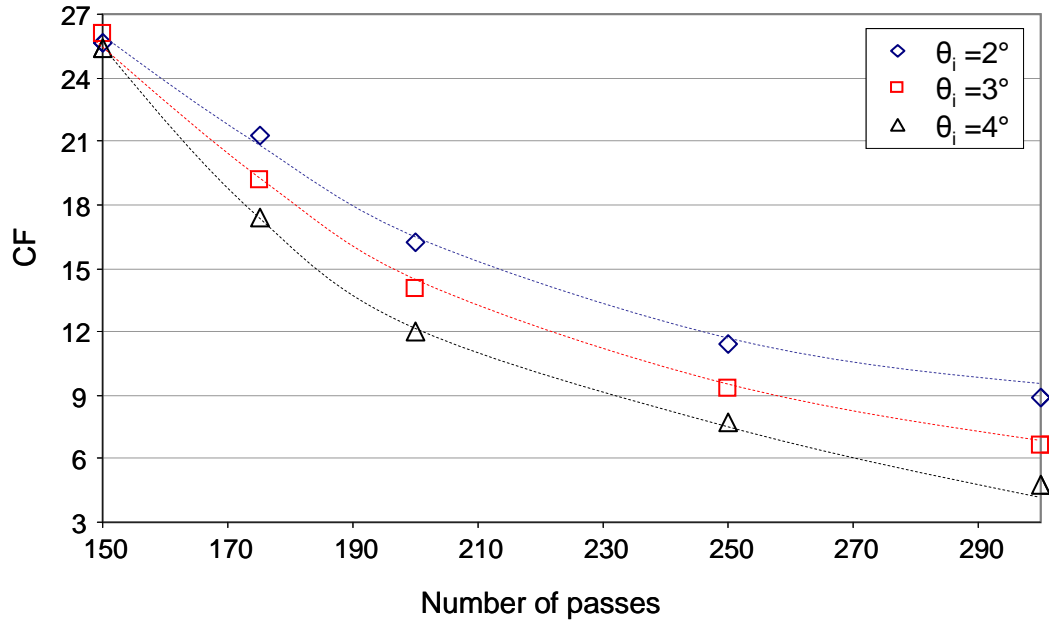


**Fig.7** – Conical factor calculated on the averaged values of figures 5 and 6 and relative variations in enlargement phase. The dashed trend-lines are just a guide for the eyes.

### 3.3 Finishing

During the finishing phase the beam rotates at the radius of 80  $\mu\text{m}$  (nominal radius minus the laser spot radius) for a certain number of passes. This ultimate phase starts with the boundary conditions (taper) generated in the enlargement phase.

A first attempt of finishing was made with the aim of verifying the ablation capability of this phase and the effects of multiple and superimposed laser passes. The main objective was to remove material at the exit of the hole without enlarging the inlet diameter, which already reached the nominal value at the end of the previous phase. Otherwise, if additional enlargement would be found at the entry side, an ablation allowance should be provided at the end of the previous enlargement phase. The process parameters adopted for the first attempt are listed in table 6.

	Values								
Parameters	Pilot-hole	Enlargement				Finishing			
Radius of rotation	Constant 10 μm	Spiral 10 μm→ 80 μm				Constant 80 μm			
Incidence Angle [°]	4.5	2				0	1	2	
Number of passes	75	100	200	250	300	100	150	200	250

Table 6 - First finishing attempt parameters. The total drilling time can be evaluated adding the number of passes for the three phases for each combination and dividing for the rotational frequency of 100 Hz.

As done before, five holes for each combinations enlargement-finishing showed in table 6 were made (48 combinations). The first finishing tests showed  $D_{\text{in}} = 180 \pm 2 \mu\text{m}$  within the range of parameters reported in table 6 meaning that repeated passes at nominal radius did not produce any enlargement of the entry side diameter whose dimension remains constant as the number of passes of the finishing phase increases.



Concerning the exit diameter, the ultimate phase was found to deeply modify the taper of the hole. Starting from a  $CF \geq 20$  tapered hole (even enlarged with 150 passes), it was possible to obtain a cylindrical hole ( $-0.5 < CF < 0.5$ ) at the end of the finishing phase. The exit edge of the holes enlarged with 100 passes showed deposits and burrs, irrespective to the number of passes or incidence angles adopted in the finishing phase. Holes enlarged with a higher number of passes did not show any sort of residuals after the finishing phase.

The graph in figure 8 shows that, being  $D_{in}$  almost constant at  $180 \pm 2 \mu m$ , the behavior of the conicity factor with process parameters is mainly governed by the dimension of the outlet diameter.

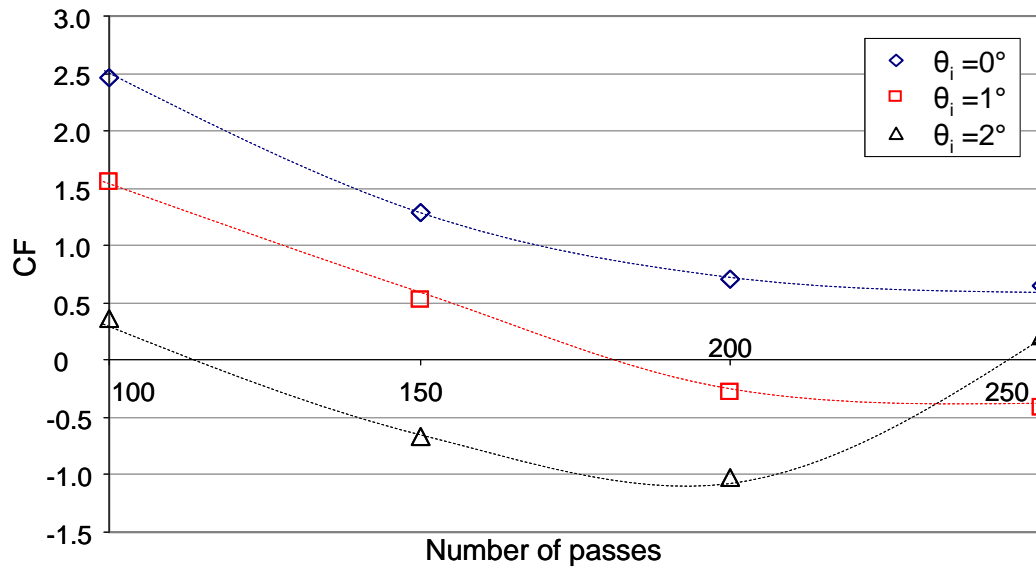


**Fig.8** – Conical factor calculated on the averaged values of the experimental data and relative variations in finishing phase. Enlargement phase obtained with 200 passes. The dashed trend-lines are just a guide for the eyes.

Looking at the behavior of  $D_{out}$  with the number of passes in the finishing phase, a general decrease in the CF can be noticed up to the value of 200. Only slight variations were induced with additional 50 passes and for  $\theta_i = 2^\circ$  an inversion in the tendency of CF was found: **increasing (even slightly)  $\theta_i$  reduces the angle with which the beam impinges of the conical inner surface generated by the enlargement phase. In these conditions more energy can be transferred to the material inside the microhole which results in the formation of melt material closing the exit diameter of hindering the beam to reach a complete ablation. As a result there's a trade off in the use of  $\theta_i$ : a sufficient value is needed in order to obtain a cylindrical shape of the hole in the minimum drilling time but increasing its value determines an increase in the energy transferred to the workpiece. This means that (for the hole geometry under consideration) the number of passes should not be increased at the same time in order to avoid the formation of burrs.**

Concerning the incidence angles, high values allowed less tapered holes with the same number of passes. The first finishing test evidenced the importance of the incidence angle on the exit diameter dimension: varying its value it was possible to ablate material at the exit position of the hole, without affecting the entry side diameter. The dimension of the exit diameter at the end of the finishing phase is then a function of both incidence angle and number of passes. Based on these results, a second trial seeking for a further minimization of the cycle time was carried out. Less number of passes in both enlargement and finishing phases were used with respect to the first attempt. Furthermore, higher incidence angles were selected in

both phases to increase the removal at the exit position of the beam in a shorter cycle time. Parameters used in the second attempt are listed in table 7.

Parameters	Values						
	Pilot-hole	Enlargement			Finishing		
Radius of rotation	Constant 10 $\mu\text{m}$	Spiral 10 $\mu\text{m} \rightarrow$ 80 $\mu\text{m}$			Constant 80 $\mu\text{m}$		
Incidence Angle [°]	4.5	2	3	4	1	2	3
Number of passes	75	150	175	200	75	100	150

Table 7 - Second finishing attempt parameters.

The second finishing tests showed that, for the hole diameter under investigation, the incidence angle cannot be increased beyond 3° without the risk of enlarging  $D_{in}$  with respect to the requested value of 180  $\mu\text{m}$ . Higher inclinations cause the laser beam to ‘touch’ on the right side of the hole (referring to figure 3.b) determining a further and unwanted ablation. This constraint in the use of the incidence angle as process parameter is determined by the aspect ratio of the microhole and can vary for different diameters or thicknesses.

High values of the incidence angle (up to 4°) in the enlargement phase allowed to produce cylindrical holes with fewer passes, because they achieved larger exit diameters at the end of the enlargement phase reducing the number of passes required to obtain a cylindrical hole at the end of the finishing phase.

All the data collected from the finishing tests were ordered based on the dimensions of the diameters and on the relative cycle time. Among all, six sets of parameters able to produce a cylindrical microhole ( $-0.5 < CF < 0.5$ ) were selected and reported in table 8.

	Pilot-hole		Enlargement		Finishing		$D_{in}$ [ $\mu\text{m}$ ]	$D_{out}$ [ $\mu\text{m}$ ]	CF	Tot. turns	Cycle time [s]
	Turns	Angle	Turns	Angle	Turns	Angle					
1	75	4.5°	150	3 °	100	2°	181.3	181.6	0.10	325	3.25
2	75	4.5°	150	4°	100	1°	180.3	182.0	0.49	325	3.25
3	75	4.5°	175	2°	75	3°	181.8	180.6	-0.46	325	3.25
4	75	4.5°	175	3°	100	2°	181.9	181.9	0	350	3.5
5	75	4.5°	200	3°	75	2°	182.0	180.9	-0.32	350	3.5
6	75	4.5°	200	2°	100	2°	181.2	179.8	-0.49	375	3.75

Table 8 – Sets of parameters selected.

### 3.4 Repeatability tests

The sets of parameters defined above in table 8 were used for a repeatability test. During this test, thirty holes for each set of parameter selected were performed. After measurements, mean values and variances of entry/out sides diameters and taper were calculated assuming a normal distribution of the measured data. The process capability was evaluated for the six sets of process parameters for each of the three output parameters:  $P(D_{in})$ ,  $P(D_{out})$ ,  $P(CF)$ . The tolerance boundaries ( $\pm 2\mu\text{m}$  for  $D_{in}$  and  $D_{out}$  and  $\pm 0.5$  for CF) were standardized according to the variances calculated for each set of parameters and the process capability was evaluated as the number of events falling inside this interval with respect to the thirty holes. The results of this calculation are shown in table 9.

Only configurations 3 and 6 were able to produce cylindrical micro-holes even though configuration 3 has a process capability in the obtainment of CF of only 56%. Process capability for configuration 6 is much higher (99%) and, assuming the distribution of measures as a standard normal distribution, it has proven to be the most repeatable since it is the only one capable to meet the requirements (cylindricity on a diameter of  $180 \pm 2 \mu\text{m}$ ) in more than 95% of cases.

Repetition test results evidenced that the variance on the dimension of the inlet diameter decreases increasing the number of passes in enlargement phase: this is probably linked to the benefits of a more stable ablation associated to small radial increments per turn in the laser trajectory. As a consequence, the variances of the outlet diameter and the conical factor show a similar trend.

	<b>D<sub>in</sub></b>		<b>D<sub>out</sub></b>		<b>CF</b>		<b>P(D<sub>in</sub>)</b>	<b>P(D<sub>out</sub>)</b>	<b>P(CF)</b>
	<b>Mean [<math>\mu\text{m}</math>]</b>	<b><math>\sigma^2</math></b>	<b>Mean [<math>\mu\text{m}</math>]</b>	<b><math>\sigma^2</math></b>	<b>Mean</b>	<b><math>\sigma^2</math></b>			
1	180.3	2.28	183.2	1.11	0.74	0.51	94.9%	41.8%	30.9%
2	179.4	1.63	183.0	1.19	1.05	0.17	95.8%	48.6%	0.05%
3	181.1	1.32	182.6	2.20	0.43	0.38	95.5%	57.0%	56.1%
4	179.8	2.21	182.8	1.96	0.86	0.37	94.0%	54.7%	18%
5	180.2	0.64	182.3	0.63	0.61	0.11	99.7%	87.2%	16.3%
6	179.9	0.36	180.4	0.60	0.10	0.07	99.9%	98.2%	99.9%

Table 9 – Results of the repeatability test.

General guidelines linking the variance of the holes characteristics with the incidence angle are difficult to derive. This is due to the geometrical constraints imposed by the relationship with the hole diameter and the beam spot size. If the hole diameter is of the same order of magnitude of the spot diameter, also using  $\theta_i=2^\circ$  in the enlargement phase may bring the beam ‘touch’ on the entry side edge opposite to the spot position. Anyhow the incidence angle was found to be an essential parameter to perform cylindrical holes: as shown during the enlargement and finishing tests, using high incidence angles allows to produce the requested shape with a significant reduction of passes (i.e. the cycle time).

#### 4. Internal quality inspection

The microholes drilled during the repeatability test were cross sectioned and inspected with Scanning Electron Microscopy with the main target to identify anomalies in the cylindrical shape of the microholes but also to check for the presence of residuals, melt layers or different defects. In fact, during the drilling tests the microholes were considered perfectly tapered and characterized by the inlet and outlet diameters dimensions only. However, differences in the ablation mechanism due to changing of the energy density with increasing depth and the beam trajectory scheduling, may lead to non-cylindrical shape: in particular, exceeding with incidence angle could produce barrel-shaped holes (larger diameter in the middle of the drilled thickness), whereas a non-correct focal position could lead to trumpet-shaped holes (larger diameter at the entry side).

Figure 9 shows a typical cross section of microholes obtained using the configuration 6: SEM inspection shows straight inner surfaces characterized by internal cleanliness and the sharpness of both entry side (fig. 9.c) and exit edges (fig. 9.b). A detailed analysis of the cross-section of the holes drilled with configuration 6 revealed a shape that can be considered cylindrical on the whole drilled thickness. Conversely, microholes obtained with higher incidence angles, especially in finishing phase, showed a barrel-shape which does not fit to the specific design of precise fluid-dynamics (e.g. nozzle drilling). The SEM analysis confirmed what previously showed by repetition tests: the use of the incidence angle as process parameter has to be tuned on the aspect ratio of the hole to be performed in order to obtain cylindrical shapes with very low variance.

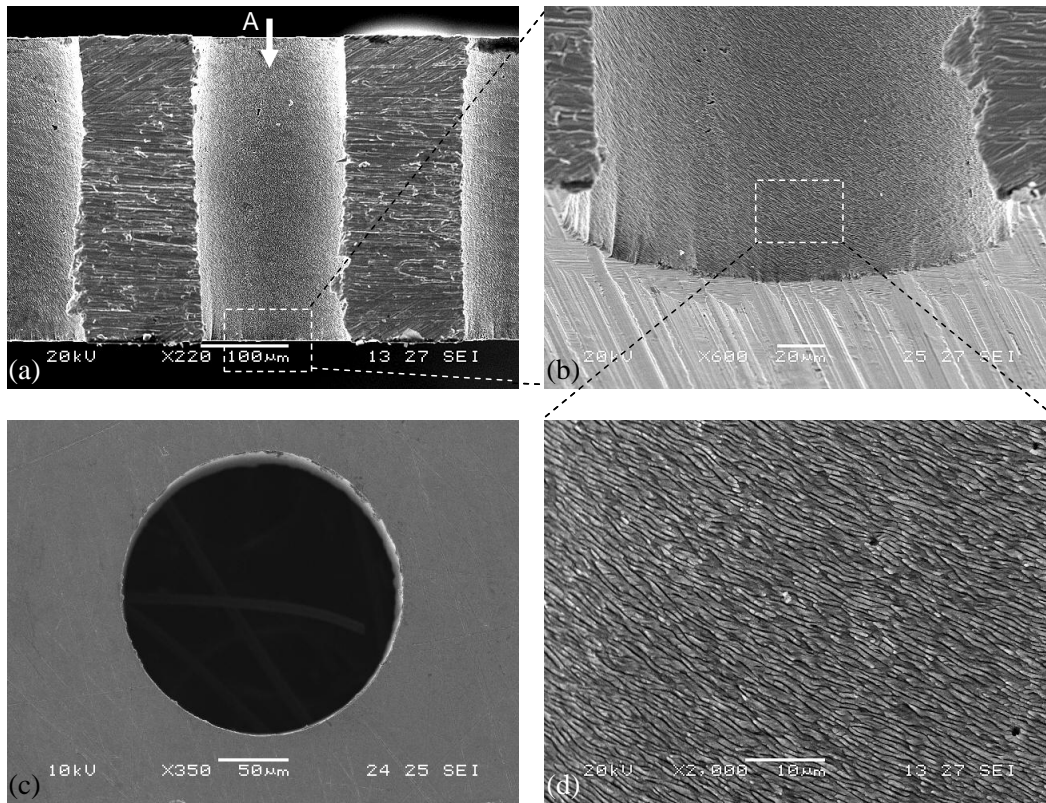


**Fig.9** – (a) Cross-section of a microhole obtained with the configuration 6 of table 8; (b) magnification of the exit edge of the microhole; (c) top view of the specimen from the direction A, showing the entry side of a microhole; (d) magnification of the inner surface of the hole showing the presence of elongated and periodic ripples.

Further magnifications on the ablated surfaces (fig.9.d) showed the presence of elongated and periodic structures which are typical of the interaction between ultrashort laser pulses and metals and often referred as Laser Induced Periodically Surface Structure (LIPSS). The strong correlation between polarization direction and ripples orientation suggests the absorbed electromagnetic field vector into the sidewall to be the main control parameter for the self-arrangement of the surface instability [24]. It is known in the literature that, circular polarization does not lead to LIPSS formation unless large  $\theta_i$  are used while elliptical polarization at normal incidence ( $\theta_i = 0^\circ$ ) generates LIPSS elongated perpendicularly to the direction of the strong field (major axis of the ellipse) [25]. Taking into account a simple approach based of Fresnel laws, the grazing incidence of the laser beam on the conical surface of the tapered hole (at the beginning of the finishing phase) has almost the same value of the

Brewster angle between air and steel (70-85° [23]): this results on the s-component of the light being reflected much more than the p-component. As a result, the strong anisotropy in the absorption at grazing incidence produces an anisotropy in the electromagnetic field absorbed by the material and the effect on LIPSS formation is similar to that obtainable by elliptical polarized light on a flat surface perpendicular to the beam axis. **Creating such anisotropy by setting the incidence angle of laser light on a predefined hole taper can be thought as a possible way to control the elongation and orientation of the ripples**, as demonstrated in [26].

**Due to high pulse overlapping in a confined space, the pilot hole phase is really far from a near-threshold ablation needed to self-rearrangement phenomena on the machined surface. The enlargement phase is characterized by ripples on the conical inner surface which are in turn destroyed and rearranged in the finishing phase. As a consequence the assumption of considering LIPSS to evolve only in the last finishing phase is not far from the experimental evidence. Nevertheless, due to different intensity distribution and different incident angle of the laser radiation on the hole internal wall at different hole depths, LIPSS inclination is not homogeneous along the hole depth: measurement revealed a maximum variation of about 5° from top to bottom.**

## 5. Conclusion

A novel micro-drilling cycle to obtain cylindrical holes on stainless steels was proposed and tested by means of experiments. The research demonstrated that subdividing the drilling process in sequential phases, each of them fulfilling specific requirements, allows to solve the trade-off between drilling time and quality, as in a route sheet for conventional manufacturing processes. Even considering the complexity of the microdrilling process and the amount of variables governing the ablation process, the drilling cycle based on a drilling through phase, an enlargement (roughing) phase and a finishing phase was able to produce cylindrical holes ( $-0.5 < CF < 0.5$ ) of  $180 \pm 2 \mu\text{m}$  of diameter on  $350 \mu\text{m}$  thick plate in total absence of burrs and debris within a drilling time of 3.75 s (nearly one fifth of the time necessary for micro-EDM). This represents a remarkable achievement in order to maximize the rate of production. The repeatability of the drilling results is extremely high (99%) meaning that the choice of parameters for the three phases ensures stable geometries which could be easily implemented in an industrial environment for the mass production of precision mechanics devices.

The experimental activity allowed to characterize the influence of each phase on the whole drilling cycle deriving guidelines for obtaining holes with pre-defined shapes and characteristics. More in detail the results can be pinpointed as follows:

- ✓ the requested cylindrical shape does not evolve in homothetic way and a pilot-hole with negative conicity factor can be easier and faster enlarged than a cylindrical one. Even small incidence angles are requested to generate such a shape with a trepanning along small radius trajectories.
- ✓ The enlargement phase is not enough to generate a cylindrical shape in any of the configuration of process parameters but, being its target only focused on maximizing the removal rate, microholes having  $CF \leq 5$  can be obtained in less than 2.5 s.
- ✓ The incidence angle is a crucial parameter to remove the material at the exit side of the microhole (bringing the CF near to zero). Increasing  $\theta_i$  shortens the finishing phase but it should not exceed the geometrical constraint given by the contact of the beam of the entry side of the hole.

The inspection of the inner surface of the microholes shows the presence of elongated and periodic ripples which testify the occurrence of a refined ablation process without any melt layer deposition. The presence of elongated and periodic ripples (LIPSS) suggests that, due to uneven light absorption, the laser polarization changes from circular to elliptical over the tapered inner surface generated during the enlargement phase.

## Acknowledgements

Marco Fiaschi, laser processing expert at Continental Automotive Italy s.p.a. is sincerely acknowledged for his support to this research. Authors are also in debt with Luciana Bertoncini (Continental Automotive Italy s.p.a.) for having provided means and facilities needed to carry out the experimental phase.

## References

- [1] Rajurkar KP, Sundaram MM, Malshe AP. Review of Electrochemical and Electrodischarge Machining. *Procedia CIRP* 2013; 6: 13-26.
- [2] Okasha MM, Mativenga PT, Driver N, Li L. Sequential laser and mechanical micro-drilling of Ni superalloy for aerospace application. *CIRP Annals - Manufacturing Technology* 2010; 59 (1): 199-202.
- [3] Klocke F, Klink A, Veselovac D, Aspinwall DK, Soo SL, Schmidt M, Schilp J, Levy G, Kruth JP. Turbomachinery component manufacture by application of electrochemical, electro-physical and photonic processes. *CIRP Annals - Manufacturing Technology* 2014; 63 (2) : 703-726.
- [4] Rashed CAA, Romoli L, Tantussi F, Fuso F, Bertoncini L, Fiaschi M, Allegrini M, Dini G. Experimental optimization of micro-electrical discharge drilling process from the perspective of inner surface enhancement measured by shear-force microscopy. *CIRP Journal of Manufacturing Science and Technology* 2014; 7: 11-19.
- [5] Lin TC, Yan BH, Huang FY. Surface improvement using a combination of electrical discharge machining with ball burnish machining based on the Taguchi method. *International Journal of Advanced Manufacturing Technology* 2001; 18 (9): 673-682.
- [6] Romoli L, Rashed CAA, Fiaschi M. Experimental characterization of the inner surface in micro-drilling of spray holes: a comparison between ultrashort pulsed laser and EDM. *Optics and Laser Technology* 2014; 56: 35 – 42.
- [7] Meijer J, Du K, Gillner A, Hoffmann D, Kovalenko VS, Masuzawa T et al. Laser machining by short and ultrashort pulses, state of the art and new opportunities in the age of photons. *CIRP-Annals – Manufacturing technology* 2002; 51 (2) : 531-550.
- [8] Hanon MM, Akman E, Genc Oztoprak B, Gunes M, Taha ZA, Hajim KI et al. Experimental and theoretical investigation of the drilling of alumina ceramic using Nd:YAG pulsed laser. *Journal of Optics and Laser Technology* 2012 ; 44: 913–922.
- [9] Ng GKL, Li L. The effect of laser peak power and pulse width on the hole geometry repeatability in laser percussion drilling. *Optics and Laser Technology* 2001; 33: 393–402.
- [10] Yao YL, Chen HL, Zhang W. Time scale effects in laser material removal: a review. *International Journal of Advanced Manufacturing Technology* 2005 ; 26 (5): 598–608.



- [11] Chichkov BN, Momma C, Nolte S, Von Alvensleben F, Tünnermann A. Femtosecond, picosecond and nanosecond laser ablation of solids. *Applied Physics A* 1996; 63 (2): 109-115.
- [12] Timur AC, Kaya U, Celik B. Parameter optimization of nanosecond laser for micro drilling on PVC by Taguchi method. *Optics and Laser Technology* 2012; 44(8): 2347-2353.
- [13] Bandhopadhyay S, Gokhale H, Sarin Sundar JK, Sundarajan G, Joshi SV. A statistical approach to determine process parameters impact in Nd:YAG laser drilling of IN718 and Ti-6Al-4V sheets. *Optics and Lasers in Engineering* 2005; 43:163–82.
- [14] Biswas R, Kuar AS, Mitra S. Multi-objective optimization of hole characteristics during pulsed Nd:YAG laser microdrilling of gamma-titanium aluminide alloy sheet, *Optics and Lasers in Engineering* 2014; 60: 1–11.
- [15] Mishra S, Yadava V. Modeling and optimization of laser beam percussion drilling of nickel-based superalloy sheet using Nd: YAG laser. *Optics and Lasers in Engineering* 2013; 51: 681-695.
- [16] Ancona A, Roeser F, Rademaker K, Limpert J, Nolte S, Tuennermann A. High speed laser drilling of metals using a high repetition rate, high average power ultrafast fiber CPA system 2008 *Optics Express* 16: 8958-8968.
- [17] Ancona A, Döring S, Jauregui C, Röser F, Limpert J, Nolte S, Tünnermann A. Femtosecond and picosecond laser drilling of metals at high repetition rates and average powers. *Optics Letters* 2009; 34, 21: 3304-3306.
- [18] Schulz W, Eppelt U, Poprawe R. Review on laser drilling: I. Fundamentals, modeling, and simulation. *Journal of Laser Applications* 2013; 25: 012006.
- [19] Arrizubieta I, Lamikiz A, Martínez S, Ukar E, Tabernero I, Girot F. Internal characterization and hole formation mechanism in the laser percussion drilling process. *International Journal of Machine Tools and Manufacture* 2013; 75: 55–62.
- [20] Yilbas BS, Akhtar SS, Karatas C. Laser trepanning of a small diameter hole in titanium alloy: temperature and stress fields. *Journal of Materials Processing Technology* 2011; 211: 1296 – 1304.
- [21] Fornaroli C, Holtkamp J, Gillner A. Laser-beam helical drilling of high quality micro holes. *Physics Procedia* 2013; 41: 661 – 669.
- [22] Kling R, Dijoux M, Romoli L, Tantussi F, Sanabria J, Mottay E. Metal micro drilling combining high power femtosecond laser and trepanning head. *Proceedings of SPIE* 2013; 86080F doi:10.1117/12.2002083.
- [23] Nolte S, Momma C, Kamlage G, Ostendorf A, Fallnich C, von Alvensleben F, Welling H. Polarization effects in ultrashort-pulse laser drilling. *Applied Physics A* 1999; 68: 563–567.
- [24] Lehr J, Kietzig AM. Production of homogenous micro-structures by femtosecond laser micro-machining. *Optics and Lasers in Engineering* 2014; 57: 121–129.
- [25] Reif J, Varlamova O, Costache F. Femtosecond Laser Induced Nanostructure Formation: Self-organization Control Parameters. *Applied Physics A* 2008; 92: 1019–1024.
- [26] Romoli L, Rashed CAA, Lovicu G, Dini G, Tantussi F, Fuso F, Fiaschi M. Ultrashort pulsed laser drilling and surface structuring of microholes in stainless steels. *CIRP Annals - Manufacturing Technology* 2014; 63 (1): 229–232.